ELSEVIER

International Journal of Mass Spectrometry 179/180 (1998) 337–348

International Journal of Mass Spectrometry

Rearrangement and dissociation of ionized 1,2-diaminoethane

G. Bouchoux[a,*], N. Choret[a], A. Milliet[a], M. Rempp[a], J.K. Terlouw[b]

[a]*Département de Chimie, Laboratoire des Mécanismes Réactionnels, UMR 7651, Ecole Polytechnique, 91128 Palaiseau Cedex, France*
[b]*Department of Chemistry, MacMaster University, 1280 Main Street West, Hamilton, Ont. L8S 4M1, Canada*

Received 5 June 1998; accepted 19 July 1998

Abstract

The chemistry of ionized 1,2-diaminoethane, $[NH_2CH_2CH_2NH_2]^{\cdot+}$, $\mathbf{1}^{\cdot+}$ is studied by means of tandem mass spectrometry techniques and molecular orbital calculations at the QCISD(T)/6-31 G*//UMP2(full)/6-31G* + ZPE level. At low internal energy $\mathbf{1}^{\cdot+}$ isomerizes into the distonic ion, $[NH_2CHCH_2NH_3]^{\cdot+}$, $\mathbf{2}^{\cdot+}$ which, further, dissociates by ammonia loss. The 1,3-hydrogen migration, $\mathbf{1}^{\cdot+} \rightarrow \mathbf{2}^{\cdot+}$, is the energy determining step of the fragmentation. Ions of higher internal energy rapidly dissociate by a simple C–C bond cleavage. As confirmed by RRKM statistical calculations, this system provides a clear example of the influence of the internal energy on the competition between rearrangement and simple bond rupture. (Int J Mass Spectrom 179/180 (1998) 337–348) © 1998 Elsevier Science B.V.

Keywords: Electron impact; 1,2-diaminoethane; Distonic ions; Ammonia loss; Ab initio molecular orbital calculations; RRKM calculations

---

1. Introduction

Several studies devoted to the chemistry of ionized 1,2-ethanediol have demonstrated the lability of the C–C bond [1–6]. Its electron impact 70 eV mass spectrum contains essentially two peaks at m/z 31 and m/z 33 (relative intensities 3/1) thus pointing to a dominant C–C bond cleavage. The behaviour of the molecular ions of low internal energy confirms this trend: the major dissociation channel of the metastable ions is the expulsion of a formyl radical to give protonated methanol, m/z 33. The mechanistic pathway proposed to explain the latter process, on both experimental and theoretical basis [5, 6], involves the formation of ion-neutral complexes [7,8] after a cleavage of the initial C–C bond, as depicted in a condensed form on Scheme 1.

From a mechanistic point of view, it was of interest to investigate the homologous diamino compounds. The most simple model structure, 1,2-diaminoethane **1**, a priori exhibits close similarities with 1,2-ethanediol. Its neutral and ionized forms may support an internal hydrogen bond, thus favouring the formation of intermediate complexes such as those presented on Scheme 1. In addition, its conventional mass spectrum (electron ionization, 70 eV) is dominated by a peak at m/z 30 corresponding to $[CH_2NH_2]^+$ ions probably resulting from a direct C–C bond cleavage.

In the present study, we report on the behaviour of ions $\mathbf{1}^{\cdot+}$ as studied by tandem mass spectrometry based techniques and high level ab initio molecular orbital calculations. RRKM statistical calculations

---

* Corresponding author.

Dedicated to Professor Fulvio Cacace in recognition of his outstanding contributions for many decades to gas-phase ion chemistry and physics.

PII S1387-3806(98)14103-9

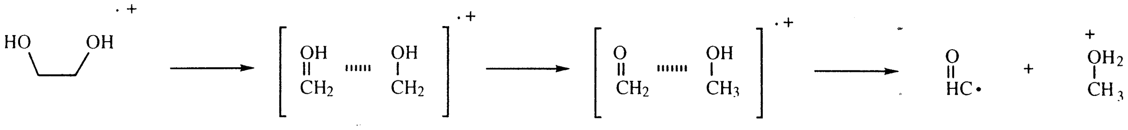

Scheme 1.

have also been performed in order to understand the differences in behaviour of ions $1^{\cdot+}$ of low or high internal energy.

2. Experimental and computational

The experiments were performed with the McMaster University VG Analytical (Manchester, UK) ZAB-R instrument of BE_1E_2 geometry (B, magnet; E, electric sector) using an accelerating voltage of 10 keV. Metastable ions (MI) mass spectra correspond to dissociations occuring in the second field free region (2ffr); collision induced dissociation (CID) mass spectra were recorded using oxygen as collision gas (transmittance, 70%). The CID mass spectra of the 2ffr metastable ions were obtained after collisions occuring in the 3ffr and scanning E_2.

Standard ab initio calculations were carried out using the Gaussian-94 series of programs [9]. Initially, the geometries of the different neutral and protonated species investigated were optimized at the UHF/6-31G* level. These geometries were then refined at the UMP2(full)/6-31G* level to take explicitly into account the effects of electron correlation. The corresponding harmonic vibrational frequencies were calculated at the same level of theory as that used for the geometry optimizations. This allowed us to verify that the stationary points found were local minima or transition structures of the potential energy surface and to calculate the zero point energy (ZPE) of the species considered. ZPEs calculated at the UMP2(full)/6-31G* level were scaled by the empirical factor of 0.966 proposed by Scott and Radom [10]. The UMP2(full)/6-31G* geometries were then utilized in single-point electronic energy calculations with the quadratic configuration interaction method. Thus our best estimates of relative energies given hereafter refer to QCISD(T)/6-31 G*//UMP2(full)/6-31G* total energies and include zero-point energy corrections.

3. Results and discussion

3.1. Experiment

As indicated before, the conventional mass spectrum of 1,2-diaminoethane, **1**, presents a dominant signal at m/z 30, corresponding to $[CH_2NH_2]^+$ ions likely originating from a simple C–C bond rupture. By contrast, the mass analyzed ion kinetic energy (MIKE) spectrum of $1^{\cdot+}$ [Fig. 1(a)] exhibits a single peak at m/z 43, associated to the loss of a molecule of ammonia. Analysis of the metastable peak shape [11] reveals a Gaussian profile associated with a relatively large release of translational energy, $T_{0,5} = 35 \pm 3$ meV (3.5 kJ/mol) and $T_{aver.} = 130 \pm 10$ meV (13 kJ/mol).

Deuterium labeling provides interesting complementary data. The MIKE spectrum of the isotopologue $[NH_2CD_2CD_2NH_2]^{\cdot+}$, **1a** (Fig. 1(b) contains two peaks at m/z 46 ($\mathbf{1a}^{\cdot+}-NH_2D$, 80% et m/z 47 ($\mathbf{1a}^{\cdot+}-NH_3$, 20%). Thus one of the hydrogen atoms of the two methylene groups partly participates in the ammonia loss. For both peaks the $T_{0,5}$ and $T_{aver.}$ values are equal to those observed for the undeuterated ion. This suggests that only one mechanism is operating in the elimination of ammonia, and that the two signals observed on the MIKE spectrum of $\mathbf{1a}^{\cdot+}$ are due to an initial hydrogen/deuterium exchange.

The CID-MIKE spectrum of ions $1^{\cdot+}$ displays intense signals at m/z 43 (70%) and m/z 30, $[CH_2NH_2]^+$ (100%). The presence of the latter peak indicates that a significant fraction of the stable ions has not undergone rearrangement after 10^{-5} s. This is

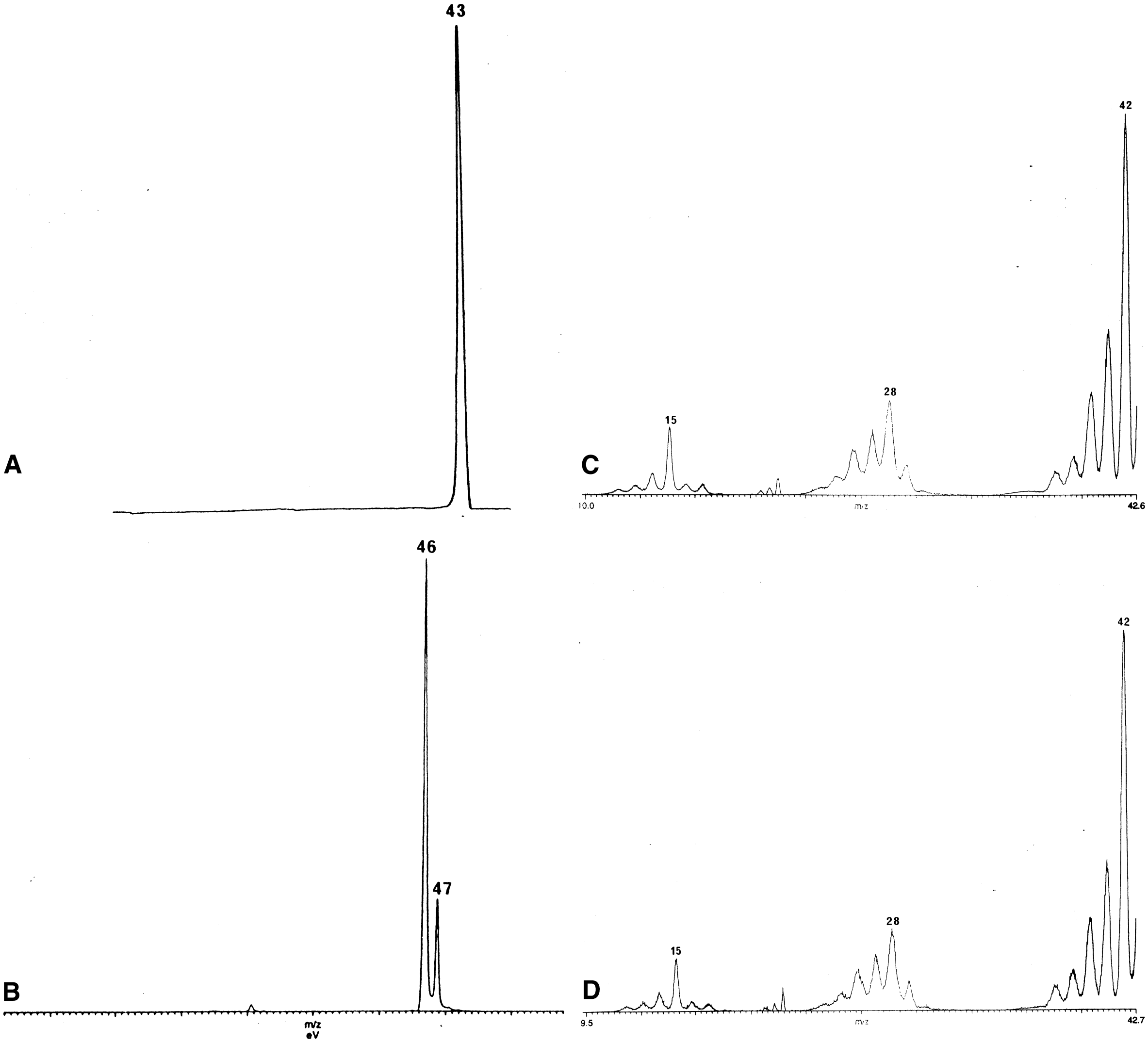

Fig. 1. Mass spectra of 1,2-diaminoethane, (A) MIKE of $\mathbf{1}^{\cdot +}$; (B) MIKE of $\mathbf{1a}^{\cdot +}$; (C) CID-MIKE of m/z 43 from metastable ions $\mathbf{1}^{\cdot +}$; (D) CID-MIKE of m/z 43 from cyclobutylamine metastable ions.

corroborated by the observation that the m/z 30 peak is cleanly shifted to m/z 32, $[CH_2NH_2]^+$, in the MIKE spectrum of $\mathbf{1a}^{\cdot +}$.

The structure of the m/z 43 ions generated by loss of ammonia from the metastable ion **1** was established by recording its CID-MIKE spectrum [Fig. 1(c)]. This spectrum appears to be identical with that of the $[M\text{-}C_2H_4]^{\cdot +}$ ions generated from metastable cyclobutylamine molecular ion [Fig. 1(d)] and this leaves little doubt that the product ions formed from $\mathbf{1}^{\cdot +}$ are ionized vinylamine, $[CH_2 = CHNH_2]^{\cdot +}$.

To summarize, the experimental data demonstrate a clear cut situation in which the dissociating species $\mathbf{1}^{\cdot +}$ undergoes a direct bond cleavage at high internal energy and a rearrangement at low internal energy. However, in contrast with 1,2-ethanediol, the rearrangement does not involve the cleavage of the C–C bond.

Table 1
Heats of formation (kJ mol^{-1}) of **1** and its possible dissociation products

X	$\Delta_f H^\circ_{300}(X)$	Ref.
1	−18	13
$\mathbf{1}^{\cdot+}$	(812)	13
$^{\cdot}CH_2NH_2$	151–159	14(d)–13
$^{+}CH_2NH_2$	745	13
$^{\cdot}CH_2NH_2 + {}^{+}CH_2NH_2$	896–904	
$CH_2 = NH$	79	14(a)
$^{\cdot}CH_2NH_3{}^{+}$	841	13
$CH_2 = NH + {}^{\cdot}CH_2NH_3{}^{+}$	920	
NCHN	(283)	14(d)
$CH_3NH_3{}^{+}$	611	13
$NCHN + CH_3NH_3^{+}$	894	
$CH_2 = CHNH_2^{\cdot+}$	838	14(b)
$CH_3CNH_2^{\cdot+}$	(919)	14(c)
$CH_3CH = NH^{\cdot+}$	(960)	14(c)
$[\text{aziridine}]^{\cdot+}$	1014	13
NH_3	−46	13
$CH_2 = CHNH_2^{\cdot+} + NH_3$	792	

3.2. Preliminary mechanistic considerations

The experimental thermochemistry relevant to the present system is summarized in Table 1.

The heat of formation of the products of the C–C bond cleavage, $[CH_2NH_2]^+ + {}^{\cdot}CH_2NH_2$, is 904 kJ/mol. In the assumption of no reverse activation barrier for this process, it is expected that the products of the ammonia loss will possess a heat of formation lower than this value. Considering the $\Delta_f H^\circ_{300K}$ value of −46 kJ/mol for ammonia, this means that the heat of formation of the corresponding m/z 43 ion should be lower than 950 kJ/mol. Only two structures are compatible with this constraint: ionized vinylamine, $[CH_2CHNH_2]^{\cdot+}$ and ionized methylaminocarbene, $[CH_3CNH_2]^{\cdot+}$. Ionized aziridine, $[\text{cyclo-}CH_2CH_2NH]^{\cdot+}$ can clearly be excluded because its heat of formation is too high. Ionized acetaldimine, $[CH_3CHNH]^{\cdot+}$, lies in an intermediate situation since its heat of formation is close to 950 kJ/mol. However, formation of this structure would imply an extensive rearrangement and this would render the reaction a weak adversary, kinetically, to the direct bond cleavage of similar energy requirement leading to the m/z 30 ions. Thus the above thermochemical arguments reinforce our evidence from the CID-MIKE spectra discussed above that the product ions are ionized vinylamine, $[CH_2CHNH_2]^{\cdot+}$.

Obviously, the most simple way to reach this product is the isomerization of the molecular ion via a 1,3-hydrogen migration, $\mathbf{1}^{\cdot+} \rightarrow \mathbf{2}^{\cdot+}$, followed by the elimination of a molecule of ammonia (Scheme 2). It is known however, that 1,3-H atom migrations are associated with high energy barrier. For example, a critical energy of no less than 132 kJ/mol has been calculated for the 1,3-hydrogen shift $[CH_3CH_2NH_2]^{\cdot+} \rightarrow [CH_2CH_2NH_3]^{\cdot+}$ [12]. 1,2- and 1,4-hydrogen migrations exhibited by the homologues, $[CH_3NH_2]^{\cdot+}$ and $[CH_3CH_2CH_2NH_2]^{\cdot+}$, require 162 and 57 kJ/mol respectively [12]. Thus, other processes involving isomeric structures $\mathbf{3}^{\cdot+}$ and $\mathbf{4}^{\cdot+}$ and one or more hydrogen migration(s) may also account for the formation of ionized vinylamine as depicted in Scheme 2.

It may be recalled at this stage that the experimental data dictate that the critical energy for the ammonia loss should be lower than that for the formation of the $[CH_2NH_2]^+$ ions. Furthermore, hydrogen migration from a carbon to a nitrogen should be irreversible since $\mathbf{1a}^{\cdot+}$ does not give elimination of ND_2H. Moreover, the hydrogen initially coming from a methylene group may exchange with the hydrogens bonded to the nitrogens since **1a** loses NH_2D and NH_3 in the ratio 80/20 (note that a statistical mixing of four H and one D would lead to losses of NH_2D and NH_3 in the ratio 60/40).

All these conditions are related to the energy levels of the isomeric forms of $\mathbf{1}^{\cdot+}$ and to the height of the barriers associated with the hydrogen migrations connecting them. To identify the lowest energy route among the various possibilities considered in Scheme 2, molecular orbital calculations were performed.

3.3. Molecular orbital calculations

The UMP2(full)/6-31G* optimized geometries and the corresponding total and relative energies are presented on Fig 2 and Table 2, respectively.

The experimentally determined enthalpy differ-

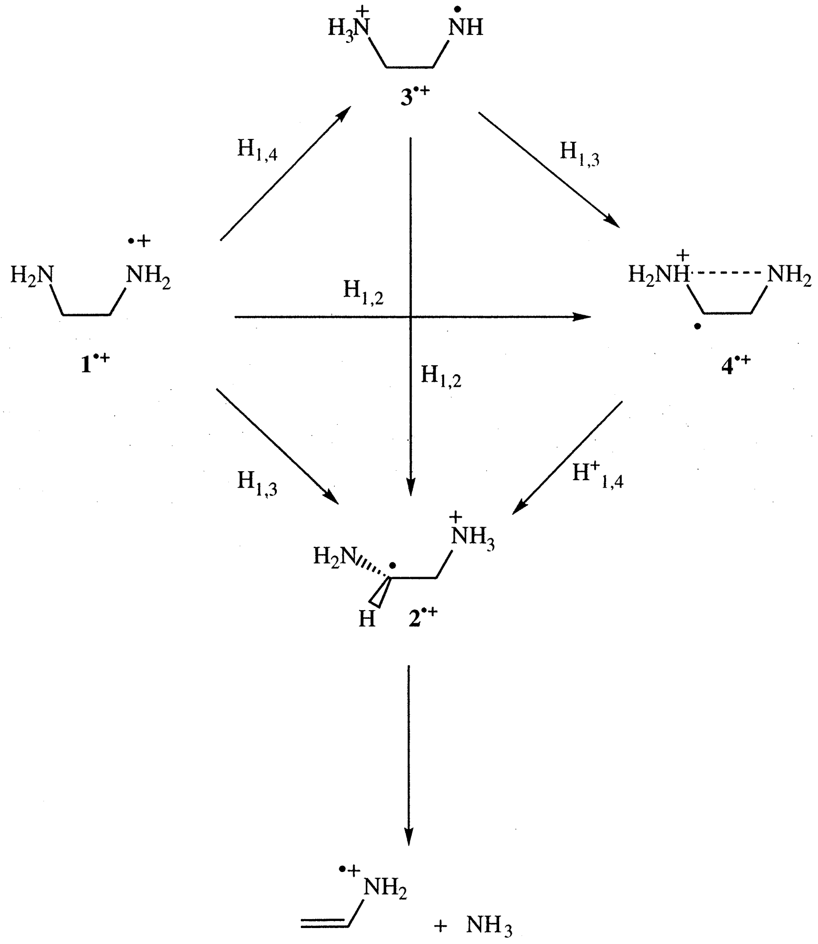

Scheme 2.

ences between the fragments $[CH_2 = NH_2]^+$ + $^{\cdot}CH_2NH_2$ and $[CH_2 = CHNH_2]^{\cdot +}$ + NH_3 (104-112 kJ/mol, Table 1) is satisfactorily reproduced by the computation (96 kJ/mol). Similarly, a difference in enthalpy of 84-92 kJ/mol is derived from the available compilation of experimental data [13] between $\mathbf{1}^{\cdot +}$ and $[CH_2 = NH_2]^+$ + $^{\cdot}CH_2NH_2$ (Table 1, note however that the tabulated heat of formation of $\mathbf{1}^{\cdot +}$ is quoted in parentheses in [13]) while the calculation indicates 117 or 107 kJ/mol depending upon the structure of $\mathbf{1}^{\cdot +}$ (the two values must be seen as adiabatic and vertical ionisation energies respectively).

3.3.1. Stable structures

At the MP2/6-31G* level of theory, two stable structures have been located for the molecular ion $\mathbf{1}^{\cdot +}$. The most stable is the trans conformer **A** which features an exceptionally large C–C bond (1.768 Å). This conformer may be seen as 1,2-diaminoethane ionized on the C–C sigma bond or as a complex between the ion $[CH_2 = NH_2]^+$ and the radical $^{\cdot}CH_2NH_2$. The second structure, **B**, enjoys an internal hydrogen bond and a NCCN dihedral angle of ca. 38°. The latter corresponds to **1** ionized on the nitrogen atom bearing the bridging hydrogen; its energy relative to **A** is 10 kJ/mol. On examining the system

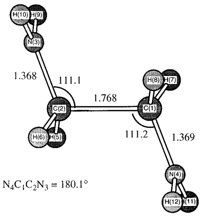

$N_4C_1C_2N_3$ = 180.1°

$1^{•+}$(A)

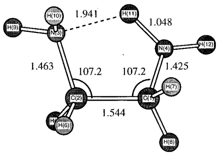

$N_4C_1C_2N_3$ = -37.8°

$1^{•+}$(B)

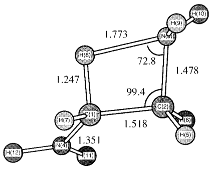

$H_8N_3C_2C_1$ = -9.5°

TS 1/2 (B/E)

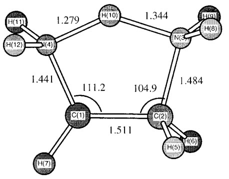

$N_4C_1C_2N_3$ = -13.4°

TS 2/4 (D/E)

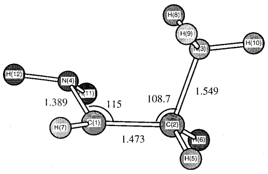

$N_4C_1C_2N_3$ = 61.8°

$2^{•+}$(E)

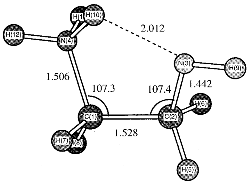

$N_4C_1C_2N_3$ = 42.4°

$3^{•+}$(C)

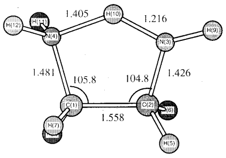

$N_4C_1C_2N_3$ = 22.9°

TS 1/3 (B/C)

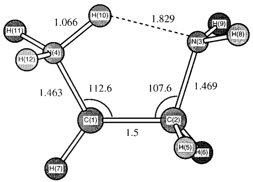

$N_4C_1C_2N_3$ = -26.5°

$4^{•+}$(D)

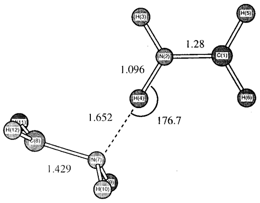

F

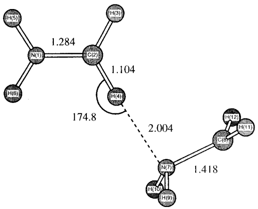

G

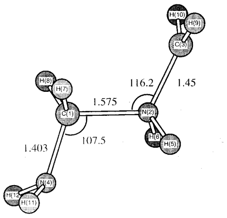

H

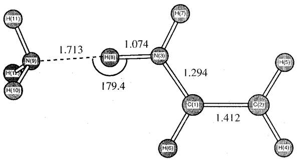

I

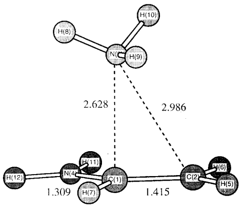

J

Fig. 2. Optimized (MP2(full)/6-31G*) stable and transition structures, selected geometrical parameters: Bond lengths in Å and bond angles in degrees.

Table 2
Total (Hartree) and relative (kJ mol^{-1}) energies calculated for various isomers and dissociation products of ionized 1,2-diaminoethane $\mathbf{1}^{\cdot+}$

	MP2(full)/6-31G*				QCISD(T)/6-31G*//MP2(full)/6-31G*		
Species	Total	Relative	ZPE[a]	+ZPE	Total	Relative	+ZPE
A	−189.597 86	0	288	0	−189.638 56	0	0
B	−189.584 57	35	284	31	−189.633 40	14	10
C	−189.597 44	1	290	3	−189.646 39	−21	−19
D	−189.596 61	3	288	3	−189.641 13	−7	−7
E	−189.608 73	−29	291	−26	−189.654 22	−41	−38
F	−189.576 91	55	274	41	−189.624 74	36	22
G	−189.561 18	96	276	84			
H	−189.583 95	37	284	33			
I	−189.599 28	−4	276	−16			
J	−189.621 51	−62	278	−72			
TS B/E	−189.553 89	115	273	100	−189.601 69	97	82
TS B/D	−189.524 55	192	275	179	−189.567 65	186	173
TS D/E	−189.592 32	15	277	4	−189.634 81	10	−1
TS B/C	−189.580 28	46	276	34	−189.627 27	30	18
TS C/D	−189.514 78	218	277	207	−189.560 45	205	194
TS C/E	−189.529 85	179	278	169	−189.573 58	171	161
$^{\cdot}CH_2NH_2$	−94.870 29		131		−94.894 55		
$^{+}CH_2NH_2$	−94.667 59		140		−94.693 11		
$^{\cdot}CH_2NH_2 + {}^{+}CH_2NH_2$	−189.537 88	157	271	140	−189.587 66	134	117
NH_3	−56.357 38		90		−56.372 08		
$CH_2 = CHNH_2$	−133.220 83		181		−133.252 00		
$NH_3 + CH_2 = CHNH_2$	−189.578 21	52	271	35	−189.624 08	38	21

[a] ZPE (corrected by a factor 0.966) in kJ mol^{-1}

further, we located minima for two ion-neutral complexes involving $[CH_2 = NH_2]^+$ and $^{\cdot}CH_2NH_2$. Both structures present a favourable interaction between hydrogen atoms of the $[CH_2 = NH_2]^+$ ion and the basic site provided by the nitrogen atom of the radical moiety. The most stable form (**F**, Fig. 2) is 22 kJ/mol less stable than **A**. It corresponds to a proton bridge involving one of the hydrogens of the amino group (the more acidic hydrogens) of the $[CH_2 = NH_2]^+$ ion. The second structure (**G**, Fig. 2) is ca. 40 kJ/mol above **F**. Finally, a distonic structure (**H**, Fig. 2) in which the initial arrangement of the CH_2 and NH_2 bonds is preserved has been located. This isomer is comparable in energy to **B**.

Hydrogen migrations from $\mathbf{1}^{\cdot+}$ may give rise to the three distonic ions $\mathbf{2}^{\cdot+}$, $\mathbf{3}^{\cdot+}$ and $\mathbf{4}^{\cdot+}$ (**E**, **C**, **D**, Fig. 2). These structures were found to be more stable than their precursor isomer **A** by 38, 19 and 7 kJ/mol respectively. Note that the most elongated C–N bond appears in $\mathbf{2}^{\cdot+}$, a situation which prefigures the dissociation into ionized vinylamine and ammonia. During the investigation of this latter process, we found several minima in the potential energy surface corresponding to ion/neutral complexes between $[CH_2 = CHNH_2]^{\cdot+}$ and NH_3. The most stable involves interaction between one hydrogen of the amino group (the most acidic) and ammonia (**I**, Fig. 2). Interestingly enough, a complex in which the electron pair of the ammonia molecule and the positively charged carbon atom of ionized vinylamine are interacting, is found to be stable (**J**, Fig. 2). The MP2/6-31G* calculation reveals energies relative to **A** of −62 and −4 kJ/mol for **I** and **J**, respectively.

3.3.2. Transition structures

Starting from $\mathbf{1}^{\cdot+}$, 1,2-, 1,3- or 1,4-hydrogen migration toward the nitrogen of one amino group may occur leading to $\mathbf{4}^{\cdot+}$, $\mathbf{2}^{\cdot+}$ or $\mathbf{3}^{\cdot+}$. Calculated critical energies with respect to $\mathbf{1}^{\cdot+}$ in the **B** conformation are equal to 163, 72 and 8 kJ/mol, respectively (Table 2). Reactions **B** → $\mathbf{4}^{\cdot+}$**(D)** and **B** → $\mathbf{2}^{\cdot+}$**(E)** are clearly 1,2- and 1,3-hydrogen atom shifts toward a cation-

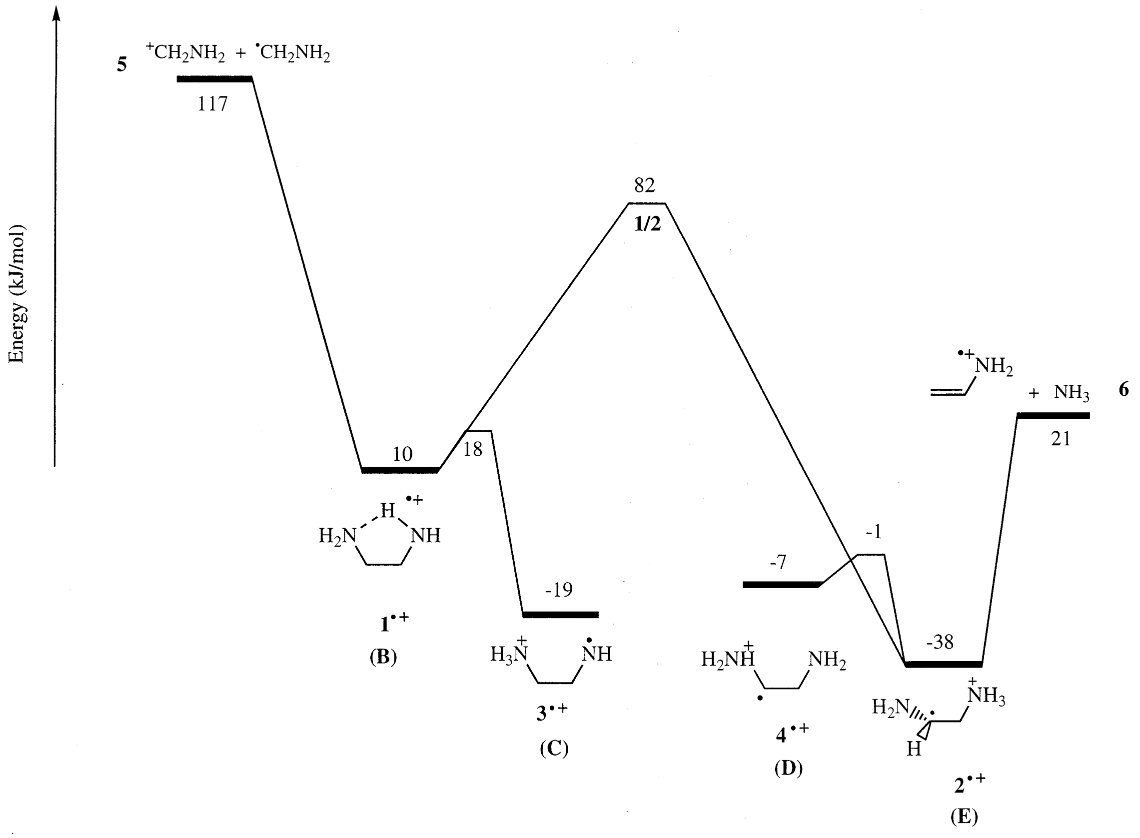

Fig. 3. Calculated potential energy profile (QCISD(T)/6-31G*//MP2/6-31G* + ZPE).

radical site. For reaction **B** → **3**$^{\cdot+}$**(C)** the migrating species is a proton rather than an hydrogen atom. The corresponding critical energies are in accordance with these characteristics.

There are two other reactions of high energy requirement: the 1,2-hydrogen atom shift **3**$^{\cdot+}$**(C)** → **2**$^{\cdot+}$**(E)** (critical energy = 161 kJ/mol) and the 1,3-hydrogen atom shift **3**$^{\cdot+}$**(C)** → **4**$^{\cdot+}$**(D)** (critical energy = 194 kJ/mol). These processes are pure hydrogen atom migrations and, accordingly, these calculated critical energies are close to that expected for an intramolecular H atom transfer in an alkyl radical [15].

Finally, reaction **4**$^{\cdot+}$**(D)** → **2**$^{\cdot+}$**(E)** is a 1,4-proton transfer for which a low critical energy is predicted (6 kJ/mol), as it was also the case for reaction **B** → **3**$^{\cdot+}$**(C)**.

3.3.3. Potential energy surface and RRKM calculations

The present calculations demonstrate that several of the elementary steps presented on Scheme 2 are not allowed to occur for ions **1**$^{\cdot+}$ of low internal energy dissociating by ammonia loss. By using the maximum limit given by the energy level of the direct dissociation products $[CH_2 = NH_2]^+ + {}^{\cdot}CH_2NH_2$, reactions **1**$^{\cdot+}$**(B)** → **4**$^{\cdot+}$**(D)**, **3**$^{\cdot+}$**(C)** → **2**$^{\cdot+}$**(E)** and **3**$^{\cdot+}$**(C)** → **4**$^{\cdot+}$**(D)** must be excluded. Moreover, the 1,3-hydrogen atom migration **1**$^{\cdot+}$**(B)** → **2**$^{\cdot+}$**(E)** appears to be the energy determining step. The corresponding QCISD(T)/6-31G*//MP2(full)/6-31G* + ZPE potential energy profile is depicted in Fig. 3.

The predictions of the ab initio model are seen to be in good agreement with the experimental observations. Initially, the passage above a high energy barrier before ammonia loss [the 1,3-H shift $\mathbf{1}^{\cdot+}\mathbf{(B)} \to \mathbf{2}^{\cdot+}\mathbf{(E)}$] is attested by the relatively large kinetic energy released during the fragmentation of metastable ions $\mathbf{1}^{\cdot+}$ and by deuterium labeling experiments (which demonstrate that the tranfer of one deuterium atom from a methylene group to a nitrogen atom in $\mathbf{1a}^{\cdot+}$ is irreversible). This is also in keeping with the conclusion, based on CID-MIKE observations, that most of the stable ions $\mathbf{1}^{\cdot+}$ are non rearranged species. The second point is the predicted reversibility of the 1,4-hydrogen migrations $\mathbf{1}^{\cdot+}\mathbf{(B)} \to \mathbf{3}^{\cdot+}\mathbf{(C)}$ and $\mathbf{4}^{\cdot+}\mathbf{(D)} \to \mathbf{2}^{\cdot+}\mathbf{(E)}$. Although the complete exchange of the N-bonded hydrogens due to the former reaction cannot be proved, the occurence of the latter is attested by the competitive losses of NH_3 and NH_2D from $\mathbf{1a}^{\cdot+}$. It was observed that the mixing of H and D atoms was not complete. This may be understood if some of the ions $\mathbf{2}^{\cdot+}\mathbf{(E)}$ resulting from the 1,3-H shift $\mathbf{1}^{\cdot+}\mathbf{(B)} \to \mathbf{2}^{\cdot+}\mathbf{(E)}$ dissociate more readily than they isomerize into $\mathbf{4}^{\cdot+}\mathbf{(D)}$. This hypothesis may be checked by considering the corresponding rate constants in the appropriate energy range. An additional question which may be answered after estimation of relevant unimolecular rate constants is: Why do ions $\mathbf{1}^{\cdot+}$ dissociate only by ammonia loss in the metastable ion regime while the simple bond fission giving $[CH_2 = NH_2]^+ + {}^{\cdot}CH_2NH_+$ is dominant at high internal energy?

These points may be investigated further by RRKM calculations of unimolecular rate coefficients [16] on the ab initio potential energy surface of Fig. 3. These were performed using the Stein-Rabinovitch algorithm [17] to estimate the sums, $[\Sigma P_{\mathbf{i}}\ddagger(E - E_0)]$ and the densities, $N_{\mathbf{j}}(E)$, of vibrations states. The normal mode frequencies given by molecular orbital calculations were used in these calculations (MP2(full)/6-31G* scaled by a factor of 0.943, torsional modes were treated as low-frequency vibrations. Table 3).

The direct fragmentation of the molecular ion $\mathbf{1}^{\cdot+}$ is associated with a single rate coefficient $k_{\mathbf{1}\,\to\,\mathbf{5}}$ given by:

$$k_{\mathbf{1}\to\mathbf{5}} = \sum P_{\mathbf{1/5}}\ddagger(E - E_{01})/h.N_{\mathbf{1}}(E)$$

Table 3
Vibrational frequencies (cm^{-1}) used in the RRKM calculations[a]

Species	1	1/2	1/5	2	2/4	2/6
	171	116	11	121	104	33
	313	285	25	234	312	119
	348	382	58	303	344	224
	435	406	137	405	597	334
	535	607	181	516	639	344
	732	640	453	580	692	400
	812	787	552	728	860	444
	857	870	871	785	876	595
	909	885	921	827	977	701
	950	963	939	906	1035	778
	973	1021	945	998	1054	950
	1061	1027	1058	1039	1060	991
	1088	1178	1114	1194	1092	1021
	1131	1193	1162	1242	1111	1218
	1227	1268	1301	1301	1267	1235
	1281	1299	1302	1327	1315	1345
	1318	1310	1411	1423	1342	1442
	1350	1431	1450	1444	1454	1538
	1392	1458	1538	1463	1584	1647
	1418	1604	1621	1606	1604	1650
	1476	1620	1699	1618	1632	1652
	1628	1697	3055	1628	1818	3068
	2827	2966	3057	2969	2942	3135
	2961	2971	3175	3056	3005	3190
	2997	3031	3177	3108	3139	3281
	3004	3334	3266	3202	3260	3364
	3024	3358	3345	3306	3326	3413
	3340	3435	3389	3335	3336	3417
	3386	3470	3445	3340	3409	3475
	3427			3454		

[a] Calculated at the MP2(full)/6-31G* level and scaled by a factor 0.9427 (see [10])

The use of a critical energy value $E_{01} = 1.11$ eV (107 kJ/mol) as indicated by the calculated QCISD(T) energy difference between $\mathbf{1}^{\cdot+}\mathbf{(B)}$ and the final state $\mathbf{5}^{\cdot+}$, leads to the $k_{\mathbf{1}\,\to\,\mathbf{5}}$ curve presented on Fig. 4.

The overall rate coefficient, $k_{\mathbf{1}\,\to\,\mathbf{6}}$, for the two steps process $\mathbf{1}^{\cdot+} \leftrightarrows \mathbf{2}^{\cdot+} \to \mathbf{6}^{\cdot+}$, is given by the steady-state expression:

$$k_{\mathbf{1}\to\mathbf{6}} = (k_{\mathbf{1}\to\mathbf{2}} \cdot k_{\mathbf{2}\to\mathbf{6}})/(k_{\mathbf{1}\to\mathbf{2}} + k_{\mathbf{2}\to\mathbf{1}} + k_{\mathbf{2}\to\mathbf{6}})$$

where the $k_{\mathbf{i}\,\to\,\mathbf{j}}$ terms represent the elementary rate constants for the $\mathbf{i} \to \mathbf{j}$ reactions.

The highest stability of $\mathbf{2}^{\cdot+}$ with respect to $\mathbf{1}^{\cdot+}$ (∼ kJ/mol) results in the inequality $k_{\mathbf{1}\,\to\,\mathbf{2}} \gg k_{\mathbf{2}\,\to\,\mathbf{1}}$. Further, for the same reason, any ion $\mathbf{1}^{\cdot+}$ of internal energy E leads to an ion $\mathbf{2}^{\cdot+}$ of internal energy $E' =$

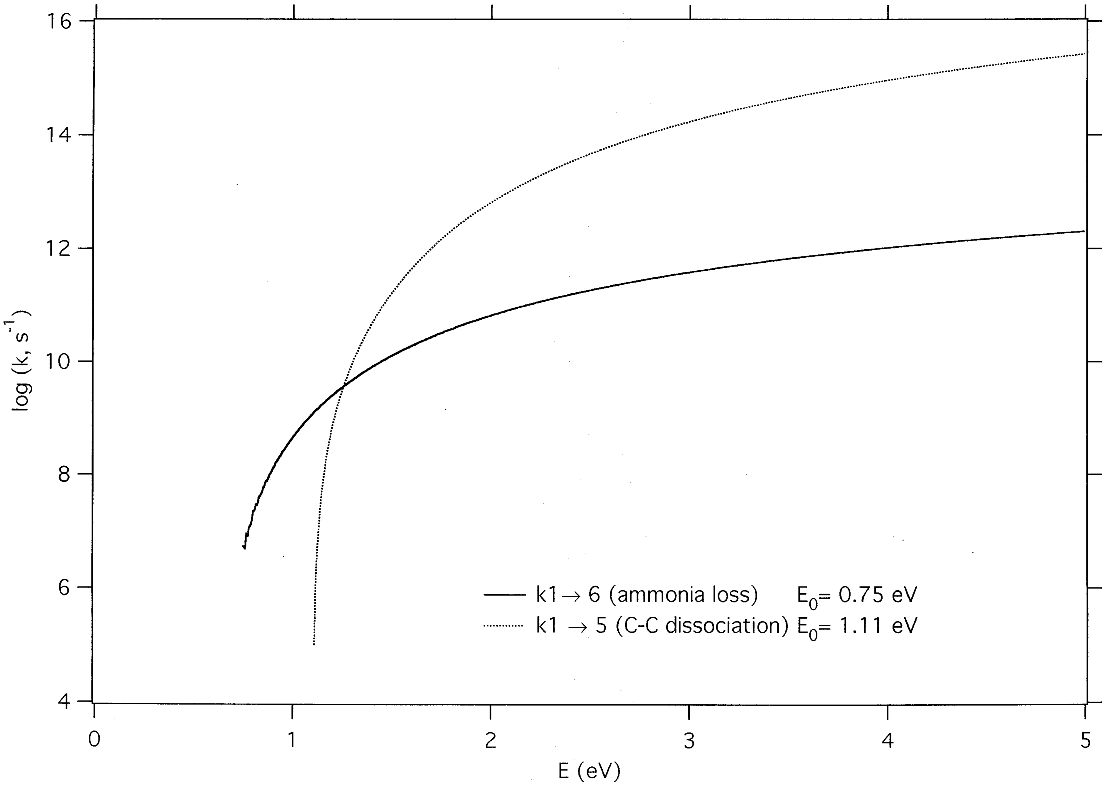

Fig. 4. RRKM rate constants for ammonia loss and simple C–C bond dissociation from $\mathbf{1}^{\cdot+}$.

$E + 50$ kJ/mol. Thus the two rate coefficients $k_{1\rightarrow 2}$ and $k_{2\rightarrow 6}$ which posses similar critical energies are in the order $k_{1\rightarrow 2} \ll k_{2\rightarrow 6}$. This is particularly true at low internal energy and is strengthered by the tightness of the transition structure **1/2** with respect to **2/6**. Consequently, to a good approximation, we can consider that:

$$k_{1\rightarrow 6} = \sum P_{1/2^{\ddagger}}(E - E_{02})/h.N_1(E)$$

The resulting rate coefficient calculated under these simplifications and using the critical energy values $E_{02} = 0.75$ eV(72 kJ/mol) is presented in Fig. 4.

As indicated by the plots depicted in Fig. 4, the calculation predicts that $k_{1\rightarrow 5}$ should be greater than $k_{1\rightarrow 6}$ at internal energies higher than $E \approx 1.3$ eV. This corresponds to rate coefficient values above 10^{10} s^{-1} i.e. to processes occuring in the ion source. In contrast, at low internal energy E, $k_{1\rightarrow 5}$ is smaller than $k_{1\rightarrow 6}$ and consequently the rearrangement reaction $\mathbf{1}^{\cdot+} \rightarrow \mathbf{6}^{\cdot+}$ predominates as experimentally observed.

Similar calculations have been undertaken for the two competitive rate coefficients $k_{2\rightarrow 4}$ and $k_{2\rightarrow 6}$. The internal energy dependences of the calculated rate coefficients for these reactions are displayed in Fig. 5. Again, one process is dominant at low internal energy, the 1,4-hydrogen migration $\mathbf{2}^{\cdot+} \rightarrow \mathbf{4}^{\cdot+}$, and another reaction, the ammonia loss $\mathbf{2}^{\cdot+} \rightarrow \mathbf{6}^{\cdot+}$, prevails at higher energy. The ions $\mathbf{2}^{\cdot+}$ generated from the reaction $\mathbf{1}^{\cdot+} \rightarrow \mathbf{2}^{\cdot+}$ possess at least an internal energy E' of 1.25 eV and Fig. 4 shows that we can reasonably assume that ions $\mathbf{2}^{\cdot+}$ coming from metastable ions $\mathbf{1}^{\cdot+}$ possess internal energy E' close to 1.25 eV. Upon examination of Figure 5, we can see that the two rate coefficients are of similar magnitude at $E' = 1.25$ eV. As suggested above, this may explain the

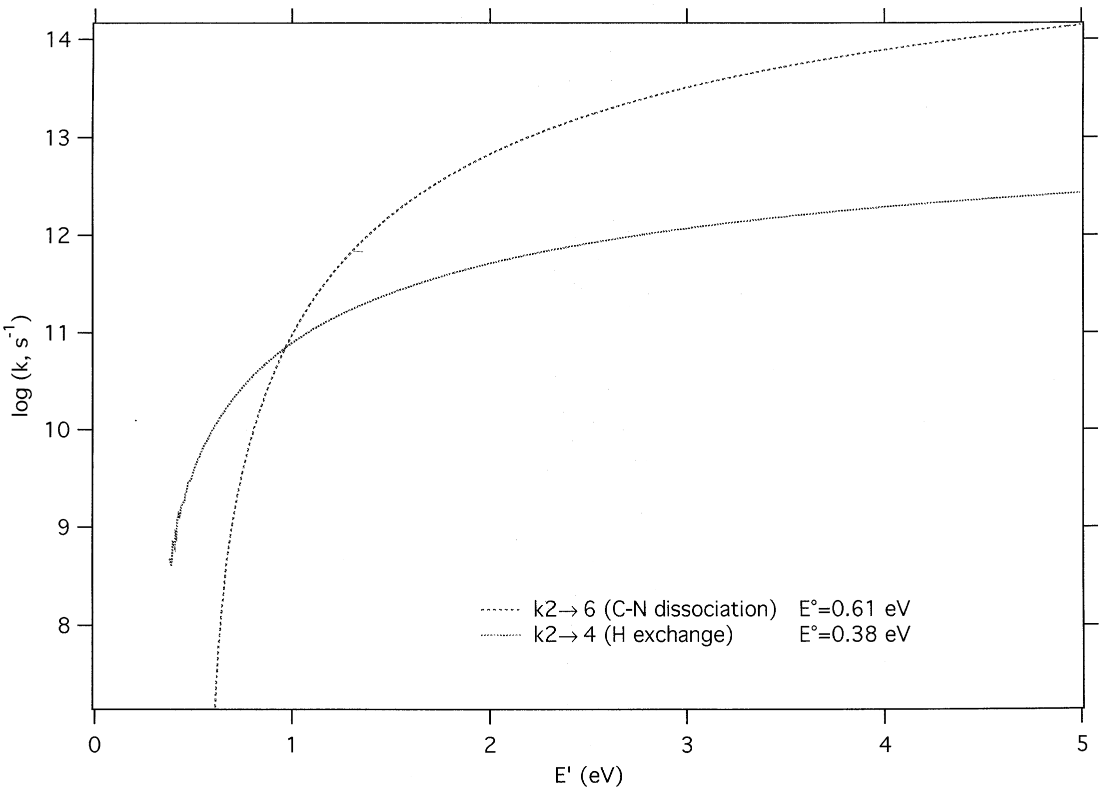

Fig. 5. RRKM rate constants for the single step reactions $\mathbf{2}^{\cdot+} \rightarrow \mathbf{4}^{\cdot+}$ and $\mathbf{2}^{\cdot+} \rightarrow \mathbf{6}^{\cdot+}$.

observation of a partial *H*/*D* mixing from metastable ions $\mathbf{1a}^{\cdot+}$ before ammonia loss.

4. Concluding remarks

The chemistry of ionized 1,2-diaminoethane, $\mathbf{1}^{\cdot+}$ is dominated, at low internal energy, by its isomerization into the distonic ion $\mathbf{2}^{\cdot+}$ and a further dissociation by ammonia loss. The various species originating from a C–C bond cleavage seem not to be operative in this energy regime. Ions of higher internal energy rapidly dissociate by a simple C–C bond cleavage. This system provides a new example of the influence of the internal energy on the competition between rearrangement and simple bond rupture.

Acknowledgements

We acknowledge the allocation of computer time at the Institut du Developpement et des Ressources en Informatique Scientifique (IDRIS, project no. 970784). J.K.T. thanks the Natural Sciences and Engineering Research Council of Canada (NSRERC) for financial support.

References

[1] P.C. Burgers, J.L. Holmes, C.E.C.A. Hop, R. Postma, P.J.A. Ruttink, J.K. Terlouw, J. Am. Chem. Soc. 109 (1987) 7315.
[2] B.F. Yates, W.J. Bouma, J.K. MacLeod, L. Radom, J. Chem. Soc. Chem. Commun. (1987) 204.
[3] J.R. Cao, M. George, J.L. Holmes, M. Sirois, J.K. Terlouw, P.C. Burgers, J. Am. Chem. Soc. 114 (1992) 2017.
[4] H.E. Audier, A. Milliet, D. Leblanc, T.H. Morton, J. Am. Chem. Soc. 114 (1992) 2020.
[5] P.J.A. Ruttink, P.C. Burgers, Org. Mass Spectrom. 28 91993) 1087.
[6] P.J.A. Ruttink, P.C. Burgers, L.M. Fell, J.K. Terlouw, J. Phys. Chem. A 102 (1998) 2976.
[7] P. Longevialle, R. Botter, J. Chem. Soc. Chem. Commun. (1980) 823.

[8] P. Longevialle, Mass Spectrom. Rev. 11 (1992) 157, and references cited therein.
[9] M.J. Frisch, G.W. Trucks, H.B. Schlegel, P.M.W. Gill, B.G. Johnson, M.A. Robb, J.R. Cheesemann, T.A. Keith, G.A. Petersson, J.A. Montgomery, K. Raghavachari, M.A. Al-Laham, V.G. Zakrewski, J.V. Ortiz, J.B. Foresman, J. Cioslowski, B.B. Stefanov, A. Nanyakkara, M. Challacombe, C.Y. Peng, P.Y. Ayala, W. Chen, M.W. Wong, J.L. Andres, E.S. Replogle, R. Gomperts, R.L. Martin, D.J. Fox, J.S. Binkley, D.J. Defrees, J. Baker, J.P. Stewart, M. Head-Gordon, C. Gonzales, J.A. Pople, Gaussian 94 Revision, Gaussian, Inc., Pittsburgh, PA 1995.
[10] A.P. Scott, L. Radom, J. Phys. Chem. 100 (1996) 16 502.
[11] J.H. Holmes, A.D. Osborne, Int. J. Mass Spectrom. Ion Phys. 23 (1977) 189.
[12] B.F. Yates, L. Radom, J. Am. Chem. Soc. 109 (1987) 2910.
[13] S.G. Lias, J.E. Bartmess, J.F. Liebman, J.L. Holmes, R.D. Levin, W.G. Mallard, J. Phys. Chem. Ref. Data. 17 (1988) (Suppl. 1).
[14] (a) G. Bouchoux, J.Y. Salpin, J. Phys. Chem. 100 (1996) 16 555. (b) G. Bouchoux, C. Alcaraz, O. Dutuit, M.T. Nguyen, Int. J. Mass Spectrom. Ion Processes 137 (1994) 93. (c) G. Bouchoux, F. Penaud-Berruyer, M.T. Nguyen, J. Am. Chem. Soc. 115 (1993) 9728. (d) D. Griller, F.P. Lossing, J. Am. Chem. Soc. 103 (1981) 1586.
[15] B. Viskolcz, G. Lendvay, T. Körtvélyesi, L. Seres, J. Am. Chem. Soc. 118 91996) 3006.
[16] T. Baer, W.L. Hase, Unimolecular Reaction Dynamic, Oxford University Press, New York, 1996, and references cited therein.
[17] S.E. Stein, B.S. Rabinovitch, J. Chem. Phys. 58 (1973) 2438.